Supramolecular Chemistry
Publication details, including instructions for authors and subscription information:
http://www.informaworld.com/smpp/title~content=t713649759

Abasic site-based DNA aptamers for analytical applications

Seiichi Nishizawa[a]; Yusuke Sato[a]; Zhiai Xu[a]; Kotaro Morita[a]; Minjie Li[a]; Norio Teramae[a]
[a] Department of Chemistry, Graduate School of Science, Tohoku University, Sendai, Japan

Online publication date: 23 June 2010

To cite this Article Nishizawa, Seiichi , Sato, Yusuke , Xu, Zhiai , Morita, Kotaro , Li, Minjie and Teramae, Norio(2010) 'Abasic site-based DNA aptamers for analytical applications', Supramolecular Chemistry, 22: 7, 467 — 476
To link to this Article: DOI: 10.1080/10610278.2010.484865
URL: http://dx.doi.org/10.1080/10610278.2010.484865

Supramolecular Chemistry
Vol. 22, Nos. 7–8, July–August 2010, 467–476

Taylor & Francis
Taylor & Francis Group

Abasic site-based DNA aptamers for analytical applications

Seiichi Nishizawa*, Yusuke Sato, Zhiai Xu, Kotaro Morita[1], Minjie Li[2] and Norio Teramae*

Department of Chemistry, Graduate School of Science, Tohoku University, Aoba-ku, Sendai 980-8578, Japan

(*Received 21 February 2010; final version received 7 April 2010*)

We here describe a class of duplex DNA aptamers that possess an abasic site as an active cavity for binding events. A structurally optimised 23-meric duplex (5′-TCT GCG TCC AGX GCA ACG CAC AC-3′/3′-AGA CGC AGG TCT CGT TGC GTG TG-5′, X = abasic site; a propyl linker, T = receptor base) binds to riboflavin with a dissociation constant of 1.9 μM (at 20°C, pH 7.0, $I = 0.11$ M), and it exhibits a high selectivity for riboflavin over flavin mononucleotide and flavin adenine dinucleotide. A fluorescent signalling aptamer is also developed by the incorporation of fluorescent 2-aminopurine (2-AP) into the duplex to flank the abasic site. This 2-AP-modified abasic site-containing duplex DNA (5′-TCTGC GTCCT PXT TAACG CACAC-3′/3′-AGACG CAGGA TCA ATTGC GTGTG-5′, P = 2-AP, X = abasic site; a propyl linker, C = receptor base) is capable of selectively binding to the bronchodilator theophylline with a dissociation constant of 10 μM (at 5°C, pH 7.0, $I = 0.11$ M), and it is applicable to monitoring serum theophylline concentrations. In addition, we describe a design strategy for label-free aptamer-based fluorescence-signalling systems based on an abasic site-binding fluorescent ligand. A DNA aptamer against adenosine is examined as a model system, and an abasic site is designed to be incorporated into the aptamer system, so that the adenosine binding causes either a release or binding of abasic site-binding ligands with a clear fluorescent signalling. The designed system is highly selective and sensitive with a detection limit of 1–2 μM for adenosine. These results are discussed as a potential basis for the further development of an aptamer-based analytical assay.

Keywords: aptamer; aptasensor; abasic site; fluorescent signalling; ligand; label free

Introduction

Aptamers, short nucleic acid-binding species, have emerged as promising candidates for molecular recognition events on account of their significant ability to bind a large number of ligands (*1–7*). High affinity and specificity of aptamers towards target ligands are generally achieved by a combination of molecular shape complementarity, hydrogen bonding and stacking interactions (*3*). Such binding events typically involve ligand-induced structural changes of the aptamers, resulting in the formation of unique secondary structures responsible for the ligand binding, of which the internal- or stem-loop structures are representative of active sites for binding events.

On the other hand, we have recently reported a relatively simple class of DNA duplex aptamers (*8*, *9*), where an abasic site (*10–14*) was utilised as an active cavity for binding events (Figure 1). While a naturally occurring abasic site is one of the most common forms of DNA damages (*10–14*), we have incorporated such lesion sites, but in a chemically stable form, into the duplex. Nucleotides constituting the active cavity were then optimised to promote ligand binding selectively and strongly by a pseudo-base pairing with an intrahelical receptor nucleobase and by stacking with nucleobases flanking the abasic site. Despite the simplicity of the binding motif, we have successfully developed a riboflavin-binding duplex aptamer with a dissociation constant K_d of 1.9 μM (at 20°C, pH 7.0, $I = 0.11$ M) (*8*). The observed binding affinity up to the micromolar range was indeed comparable with binding affinities of flavin-binding RNA aptamers (*15–18*) developed earlier by the systematic evolution of ligands by the exponential enrichment (SELEX) method. We have also developed a signalling aptamer for theophylline detection, for which a fluorescent adenine analogue, 2-aminopurine (2-AP), is incorporated into the duplex to flank the abasic site (*9*). This signalling aptamer showed highly selective response to theophylline with a useful binding affinity (10 μM at 5°C, pH 7.0, $I = 0.11$ M), and it is applicable to the detection of theophylline in serum samples.

In this paper, we review such promising binding and sensing functions of the abasic site-based DNA aptamers (*8*, *9*). Besides, combination use of an abasic site-containing DNA and abasic site-binding fluorescent

*Corresponding authors. Emails: seinishi@mail.tains.tohoku.ac.jp; teramae@mail.tains.tohoku.ac.jp.
[1]Present address: Division of Material Chemistry, Graduate School of Natural Science and Technology, Kanazawa University, Kakuma, Kanazawa 920-1192, Japan.
[2]Present address: Chemical Engineering and Technology, College of Chemistry and Chemical Engineering, Qiqihar University, Qiqihar, P.R. China.

ISSN 1061-0278 print/ISSN 1029-0478 online

DOI: 10.1080/10610278.2010.484865
http://www.informaworld.com

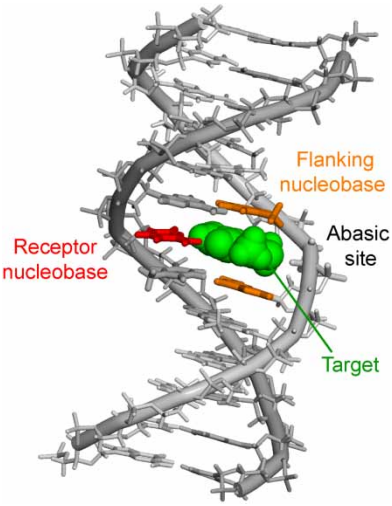

Figure 1. Illustration of the binding motif of an abasic site-containing DNA duplex as an aptamer for small ligands.

ligands is described as a basis for the design of label-free aptamer-based fluorescence-signalling systems (*19*, *20*).

Abasic site-containing duplex DNA for riboflavin binding

The first example of the abasic site-containing DNA aptamer is for riboflavin (vitamin B_2, Figure 2(A)) (*8*), a biological redox cofactor essential for human and animal health due to its crucial role in metabolism (*21*, *22*). By optimising structural parameters such as the receptor nucleotide, the length of duplexes and the flanking nucleotides to the abasic site, a 23-mer duplex DNA containing thymidine as a receptor nucleotide (**23T**: 5′-TCT GCG TCC AGX GCA ACG CAC AC-3′/3′-AGA CGC AGG TCT CGT TGC GTG TG-5′, X = abasic site, T = receptor base) is found to strongly recognise riboflavin with a 1:1 binding stoichiometry. The binding affinity of **23T** for riboflavin reaches 1.9 μM (at 20°C, pH 7.0, $I = 0.11$ M), which is comparable to the binding affinities of the previously identified flavin-binding RNA aptamers, in which the formation of the loop structure (*15*, *16*), intramolecular G-quartet (*17*) or internal bulges (*18*) was responsible for the flavin binding. While these flavin-binding RNA aptamers did not discriminate between flavin analogues, the aptamer **23T** is found to show clear binding selectivity for riboflavin over flavin mononucleotide (FMN) and flavin adenine dinucleotide (FAD). In this section, these features of the riboflavin–duplex interactions are described as a potential basis of abasic site-containing duplex DNA aptamers.

First, the effect of nucleobases opposite the abasic site on the riboflavin–duplex interactions was examined by means of melting temperature (T_m) measurements. For this, we prepared four kinds of 11-mer duplexes that contain guanine (**11G**), adenine (**11A**), cytosine (**11C**) or thymine (**11T**) as the respective receptor nucleobase for binding with riboflavin. The sequences of these duplexes are given in Figure 2(B), together with those of other duplexes (**23C**, **23T**, **41T** and **51T**) that are discussed later.

As shown in Table 1, the changes in T_m strongly depend on the nucleobase opposite the abasic site. In solutions buffered to pH 7.0 ($I = 0.11$ M), the largest change in T_m value is observed for the 11-mer duplex containing thymine base as the receptor (**11T**), for which the T_m value of the duplex (30 μM) increases by 4.0°C in the presence of riboflavin (46 μM). An increase in T_m value is also observed for the cytosine-containing duplex **11C** (+2.0°C), but it is not as significant as that for **11T**. By contrast, the ΔT_m values are almost negligible when the receptor nucleobases are adenine (**11A**: −0.5°C) or guanine (**11G**: −0.7°C). Apparently, among these four kinds of 11-mer duplexes, the thermal stability of **11T** is effectively increased in the presence of riboflavin, indicating that riboflavin is incorporated into the abasic site. The strongest binding with riboflavin is therefore expected when the receptor nucleobase opposite the abasic site is thymine.

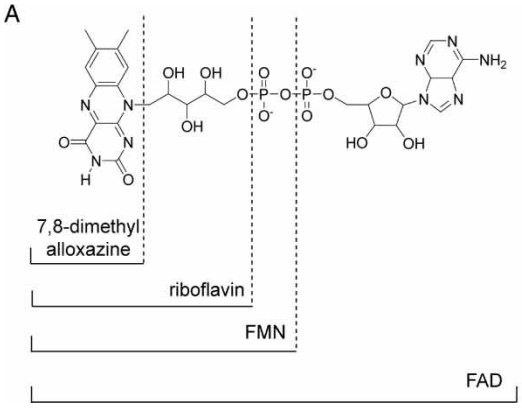

B

11G: 5′-TCC AGX GCA AC-3′
3′-AGG TCG CGT TG-5′

11C: 5′-TCC AGX GCA AC-3′
3′-AGG TCC CGT TG-5′

11A: 5′-TCC AGX GCA AC-3′
3′-AGG TCA CGT TG-5′

11T: 5′-TCC AGX GCA AC-3′
3′-AGG TCT CGT TG-5′

23C: 5′-TCT GCG TCC AGX GCA ACG CAC AC-3′
3′-AGA CGC AGG TCC CGT TGC GTG TG-5′

23T: 5′-TCT GCG TCC AGX GCA ACG CAC AC-3′
3′-AGA CGC AGG TCT CGT TGC GTG TG-5′

41T: 5′-CAG CCG ATA ACG AAG TCC AGX GCA ACG ACA CGC ATA TGT GC-3′
3′-GTC GGC TAT TGC TTC AGG TCT CGT TGC TGT GCG TAT ACA CG-5′

51T: 5′-GTG ACA CGC GAT TAA GAC AGT CCA GXG CAA CGC ACA CCA ATG CAA GGT CCA-3′
3′-CAC TGT GCG CTA ATT CTG TCA GGT CTC GTT GCG TGT GGT TAC GTT CCA GGT-5′

Figure 2. (A) Chemical structures of 7,8-dimethylalloxazine, riboflavin, FMN and FAD. (B) Names and sequences of duplex DNAs examined in this study: X = abasic site (Spacer-C3, a propyl linker), N = receptor base.

Table 1. Melting temperatures (T_m/°C) for the aptamers in the absence and presence of riboflavin[a].

Aptamer	$T_{m(-)}$	$T_{m(+)}$	ΔT_m
11G	34.6	33.9 (±0.1)	−0.7
11A	33.9	33.4 (±0.1)	−0.5
11C	30.9	32.9 (±1.0)	+2.0
11T	29.1	33.1 (±0.8)	+4.0

[DNA] = 30 μM; [riboflavin] = 46 μM; heating rate, 1.5°C/min; $T_{m(-)}$, melting temperature of riboflavin-free DNA and $T_{m(+)}$, melting temperature of the DNA with riboflavin added, $\Delta T_m = T_{m(+)} - T_{m(-)}$.
[a] T_m measurements were done in solutions buffered to pH 7.0 (10 mM sodium cacodylate) containing 100 mM NaCl and 1.0 mM EDTA.

The binding affinity of the 11-mer duplexes with riboflavin was further examined quantitatively by fluorescence titration experiments, for which the binding-induced changes in the fluorescence of riboflavin were utilised. While riboflavin (1.0 μM) shows no obvious changes for the normal 11-mer duplexes containing no abasic sites (2.0 μM, 5′-TCC AGA GCA AC-3′/3′-AGG TCT CGT TG-5′), its fluorescence is significantly quenched in the presence of abasic site-containing duplexes (2.0 μM). In accordance with the T_m measurements, the largest quenching is observed when the receptor nucleobase at the abasic site is thymine (**11T**), followed by cytosine (**11C**), adenine (**11A**) and guanine (**11G**). For all cases, the resulting changes in fluorescence spectra can be explained by the formation of a 1:1 complex, and a dissociation constant K_d (at 20°C, pH = 7.0, I = 0.11 M) follows in the order of **11T** (5.0 μM) <**11C** (12 μM) <**11A** (77 μM) <**11G** (303 μM). For effective binding with riboflavin, thymine is therefore the most suitable nucleobase as the receptor in the abasic site-containing duplex.

Interestingly, the binding affinity for riboflavin is further strengthened by the use of longer duplexes. The binding affinity with the 23-mer duplex containing thymine opposite the AP site, **23T** (Figure 2(B)), reaches 1.9 μM (at 20°C, pH = 7.0, I = 0.11 M), which is at least two times stronger than that with the corresponding 11-mer duplex, **11T** (5.0 μM). Similarly, the 1:1 binding affinity with the 23-mer duplex **23C** (5.0 μM) is stronger than its shorter counterpart, **11C** (12 μM). On a further increase in the duplex length, from 23-mer to 51-mer, however, the lowering trend in K_d values is rather insignificant (**41T**: 1.5 μM, **51T**: 1.9 μM), so the use of longer duplexes is not necessary. We also examined the influence of the nucleobases flanking the abasic site on the riboflavin binding with 16 variants of **23T** (–N<u>X</u>N′–, <u>X</u> = abasic site), and found that the strongest binding was obtained when the nucleobases flanking the abasic site were guanines (–G<u>X</u>G–). We, therefore, conclude that the 23-mer duplex **23T** qualifies as an ideal aptamer in our investigations.

An interesting feature of the present DNA aptamer compared to those with the previous flavin-binding RNA aptamer (*15*, *16*) is the difference in receptor nucleotides

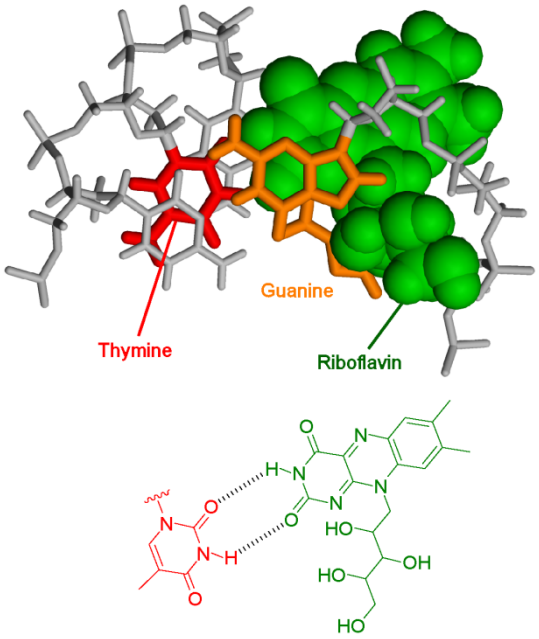

Figure 3. Possible binding mode of the riboflavin–thymine complex in **23T**, obtained using MacroModel Ver. 8.5 (*8*). The Corey–Pauling–Koltun (CPK) model for riboflavin is shown in green, receptor thymine in red and guanine flanking the abasic site in yellow. Pseudo-base pairing of thymine with riboflavin is also shown (colour online).

responsible for effective binding with riboflavin. The 3D structure of the FMN-binding RNA aptamer has been determined by NMR (*16*), and has revealed that an adenine coplanar with the flavin recognises the polar groups along the edge of the isoalloxazine ring through two hydrogen bonds. By contrast, in the present case, as is evident from the melting temperature and fluorescence studies, a thymidine moiety locating opposite the abasic site works as an effective receptor for the riboflavin binding. ^{1}H NMR measurements reveal the formation of hydrogen bonding between the receptor thymine base and riboflavin (*8*), and it is likely that at the abasic site a pseudo-base pair is formed with a thymine base along the uracil-like edge of the isoalloxazine ring of riboflavin, as shown in the energy minimised structure of the complex obtained by molecular modelling studies (Figure 3). From the calculated structure (Figure 3), we also see that the isoalloxazine ring penetrates into the abasic site, in which the flat ring moiety stacks with two adjacent guanine bases. It is, therefore, likely that the riboflavin binding of the present DNA aptamer is promoted by a combination of stacking and hydrogen-bonding interactions.

This kind of combination of molecular interactions is a common theme in aptamer complexes with flat ligands such as theophylline or AMP (*3*), and has also been observed in the ligand-binding pockets of the FMN–RNA complex. Again, the NMR structure of the FMN–RNA

Table 2. Dissociation constants K_d (μM) of the flavin-binding aptamers.

	23T[a]	FMN-2[b]	35FMN-2[b]	FAD-1[b]	27FAD-1[b]
FAD	40	1.4	0.7	137	273
FMN	49	0.5	0.5	84	280
Riboflavin	1.9	–	–	–	–
7,8-Dimethylalloxazine	0.062[c]	0.5	0.3	23	35

[a] The K_d values determined by fluorescence titration (at 20°C, pH = 7.0, I = 0.11 M) (*8*).
[b] The K_d values determined by affinity chromatography (*15*).
[c] The K_d values of **11T** determined by fluorescence titration (at 5°C, pH = 7.0, I = 0.11 M) (*48*).

complex (*16*) has revealed that, in addition to two hydrogen bonds between adenine and the isoalloxazine ring, the binding is based on stacking with the aromatic, planar platform; the stacking surface is constituted by a triple of coplanar bases (A:U:G), which lies parallel and adjacent to the bound FMN. As compared to such binding pocket isolated by *in vitro* selection, the abasic site of the present DNA aptamer is a much simpler binding pocket constituted by minimal nucleotides to provide stacking and hydrogen-bonding interactions. However, the binding affinity of **23T** up to the micromolar range (K_d = 1.9 μM) is indeed comparable to those of the RNA aptamers developed earlier for flavins (K_d = 50–0.5 μM) (*15–18*), and is significantly better than the millimolar affinity of polymer-bound zinc(II) azamacrocycles for riboflavin (K_d = 1.2 mM) (*23*). In addition, the aptamer **23T** shows a clear binding selectivity for riboflavin over FMN and FAD.

As given in Table 2, the riboflavin-binding aptamer **23T** shows a 20-fold lower affinity for FMN (K_d = 49 μM) and FAD (K_d = 40 μM), and a much stronger binding affinity is obtained for 7,8-dimethylalloxazine (K_d = 0.062 μM) that has no substitutions at N10. Such binding discrimination was not obtained by RNA aptamers previously identified for the flavin binding. While the FAD-binding RNA aptamer based on a stem-loop structure (FAD-1 and 27FAD-1) showed moderate binding selectivity, the FMN-binding RNA aptamer containing an internal-loop structure (FMN-2 and 35FMN-2) was not able to distinguish between these flavin analogues (*15*). Similarly, the RNA aptamer with the intramolecular G-quartet (K_d = 1–5 μM) (*17*) or with the several internal bulges (K_d = 50 μM) (*18*) bound to these flavins (riboflavin, FMN and FAD) with equal affinity. The aptamer **23T** is therefore structurally and functionally distinct from these previously identified flavin aptamers.

In addition to such promising binding functions, the abasic site-based DNA aptamer may have some advantages, such as its easy and low-cost synthesis and higher chemical stability, as compared with typical RNA aptamers. These features of the abasic site-based DNA aptamer would allow various kinds of analytical applications, including the isolation of riboflavin from natural sources (*23*) and the determination of riboflavin in aqueous samples (*24–26*). Moreover, our system can also be applied to the analysis of thymidine-related single-nucleotide polymorphisms (SNP), for which riboflavin (and/or its derivatives) functions as a thymidine-selective fluorescent ligand and the binding-induced quenching of its fluorescence is utilised to detect the single-base mutation (*27*, *28*).

2-AP-modified abasic site-containing duplex DNA for selective detection of theophylline

One of the keys in aptamer chemistry is to transduce binding events to detactable signals (*4–7*). In this section, we describe a signalling abasic site-based DNA aptamer in which a fluorescent adenine analogue, 2-AP, is incorporated into the duplex to flank the abasic site (Figure 4(A)) (*9*). The fluorescence of 2-AP is very sensitive to its environment, and therefore, 2-AP has been extensively used as a probe for local structure and dynamics in DNA (*29–31*). In the present aptamer, less-stacked 2-AP

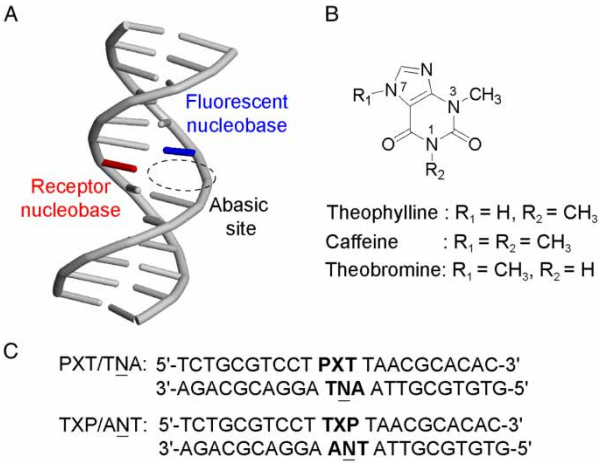

Figure 4. (A) Illustration of a fluorescent signalling aptamer based on abasic site-containing duplex DNA. (B) Chemical structures of theophylline and its derivatives. (C) Names and sequences of duplex DNAs examined in this study: P = 2-AP, X = abasic site (Spacer-C3, a propyl linker) and N = receptor base (G, C, A or T).

adjacent to the abasic site becomes more stacked with neighbouring bases and/or ligands upon binding, and the stacking causes quenching of 2-AP. Herein, we present such a fluorescent signalling aptamer that targets theophylline (Figure 4(B)), a drug for diseases such as bronchial asthma and bradycardia (*32*).

The design strategy utilised here is relatively simple, focusing on the examination of (i) the nucleobases flanking 2-AP, (ii) the position of 2-AP and (iii) the receptor nucleobases opposite the abasic site. It has been demonstrated that 2-AP exhibits quenching when stacked in duplex DNA and that guanine causes the strongest quenching of 2-AP (*29*, *30*). This indicates that the AT base pair would be suitable as the nearest-neighbour base in order to minimise the quenching of 2-AP in the uncomplexed duplex. It has also been reported that the fluorescence intensity of 2-AP adjacent to the abasic site in duplex DNA depends on its relative position (5′ or 3′) (*31*), indicating that the difference in position of 2-AP would be crucial for effective signalling. From these considerations, we prepared two series of 23-mer duplexes having 2-AP on the 5′ or 3′ side of the abasic site and a different nucleobase (G, C, A or T) opposite the abasic site (Figure 4(C)). In these duplexes, 2-AP is flanked by thymine, and the sequence of the other region is identical to that of the 23-mer duplex (**23T**) previously discussed for riboflavin binding (*8*).

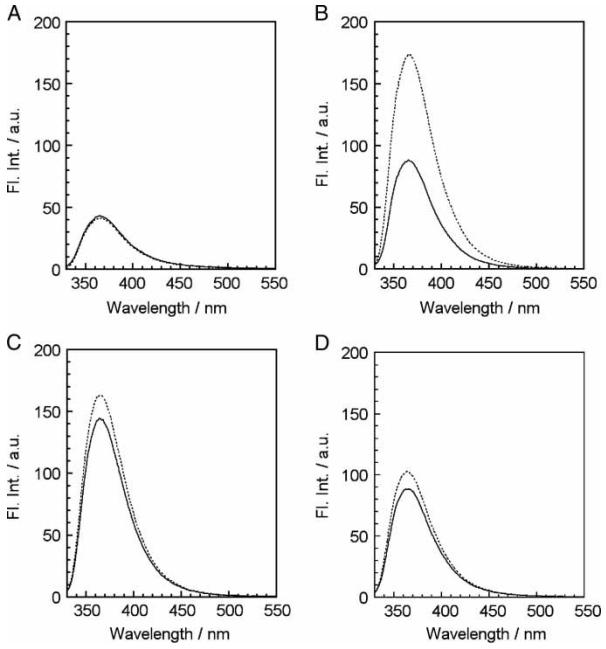

Figure 5. Fluorescence spectra of duplex DNAs (5.0 μM) having 2-AP on the 5′ side of the abasic site, in the absence (dashed line) and presence (solid line) of theophylline (200 μM): (A) PXT/TGA, (B) PXT/TCA, (C) PXT/TAA and (D) PXT/TTA (*9*). Sample solutions were buffered to pH 7.0 with 10 mM sodium cacodylate, containing 100 mM NaCl and 1.0 mM EDTA. Excitation was at 320 nm and $T = 5$°C.

First, fluorescence spectra of duplexes having 2-AP on the 5′ side of the abasic site [5.0 μM, PXT/TNA, N = receptor base (G, C, A or T)] were examined in the presence and absence of theophylline (200 μM) in solutions buffered to pH 7.0 (5°C, $I = 0.11$ M). For all of the duplexes, emission due to 2-AP with a maximum at 367 nm was observed, but the fluorescence intensity and response were strongly dependent on the receptor bases opposite the abasic site. As shown in Figure 5, PXT/TGA, with guanine as the receptor base, exhibits the weakest emission, and almost no response is observed even in the presence of 40 equiv. of theophylline. Similarly, the response to theophylline is only moderate for PXT/TAA and PXT/TTA. On the other hand, an effective quenching is observed for PXT/TCA having cytosine as the receptor base (see also Figure 6(A)), and uncomplexed PXT/TCA exhibits the strongest emission among these duplexes. It is therefore highly likely that theophylline binding takes place when cytosine is placed opposite the abasic site, and this also benefits minimum quenching of 2-AP in the uncomplexed duplex.

Similar results were obtained for duplexes having 2-AP on the 3′ side of the abasic site [TXP/ANT, N = receptor (G, C, A or T)]. Again, an effective quenching response to theophylline was obtained by TXP/ACT having cytosine as a receptor base, and its emission (λ_{max}, 367 nm) was the strongest among the four duplexes in the uncomplexed form (not shown). The observed quenching up to 45% obtained for TXP/ACT is almost comparable to the response obtained for PXT/TCA having 2-AP on the 5′ side (50%). However, the intensity of uncomplexed TXP/ACT is significantly lower than that of PXT/TCA (the ratio of the fluorescence intensities at 367 nm, $F_{TXP/ACT}/F_{PXT/TCA} = 0.45$), which is a disadvantage for the sensor application. We therefore qualified PXT/TCA as an aptamer for further investigations.

An examination of the binding affinity and selectivity reveals a promising feature of PXT/TCA for theophylline detection. As shown in Figure 6(A), the response of PXT/TCA to theophylline is concentration dependent, which is explained by 1:1 binding with a dissociation constant K_d of 10 ± 1.0 μM (Figure 6(B), $n = 3$). Significantly, PXT/TCA exhibits almost no responses to either caffeine or theobromine (Figure 6(B)), each of which differs from theophylline only by a single methyl group attached to the xanthine ring (Figure 4(B)). In addition, the responses to other substrates such as uric acid and creatinine, present in serum, are only moderate or negligible (Figure 6(B)). Apparently, PXT/TCA does work as a signalling aptamer with a high selectivity for theophylline.

The highly selective binding to theophylline over caffeine and theobromine is a distinguishing feature and is similar to that of the theophylline-binding RNA aptamer (*33*, *34*) developed by the SELEX process. This 33-mer

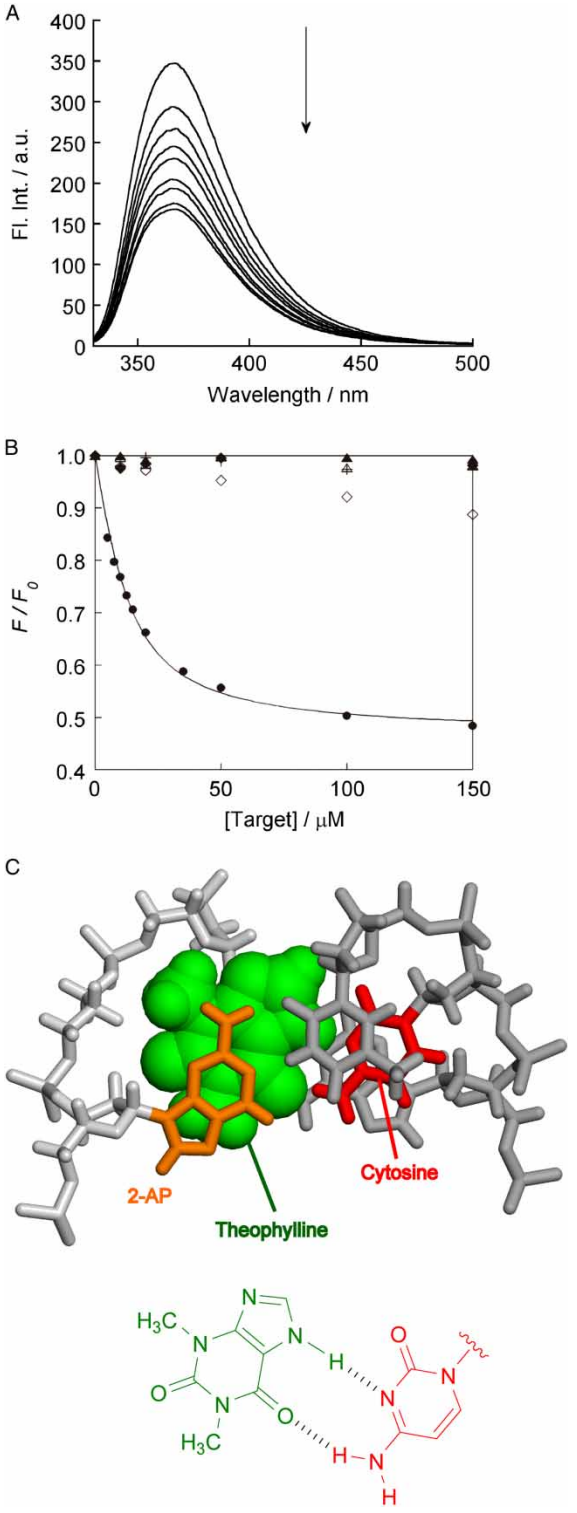

Figure 6. (A) Fluorescence response of PXT/TCA (10 μM) to theophylline (0–150 μM) in solutions buffered to pH 7.0 (10 mM sodium cacodylate) containing 100 mM NaCl and 1.0 mM EDTA (*9*). Excitation was at 320 nm and $T = 5$°C. (B) Responses of PXT/TCA (10 μM) to (●) theophylline, (Δ) caffeine, (+) theobromine, (◇) uric acid, (▲) creatinine and (◆) glucose (*9*). F and F_0 denote the fluorescence intensities (367 nm) in the presence and absence of ligands, respectively. (C) Possible binding mode of the theophylline–cytosine complex in PXT/TCA obtained using MacroModel Ver. 9.0 (*9*). CPK model for theophylline is shown in green, 2-AP in yellow and cytosine in red. Pseudo-base pairing of cytosine with theophylline is also shown (colour online).

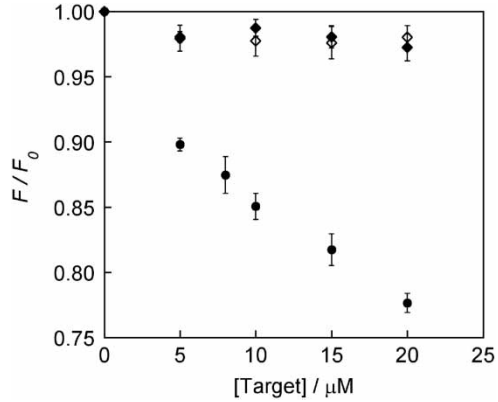

Figure 7. Detection of theophylline (●) in horse serum by PXT/TCA (*9*). The responses to caffeine (◆) and theobromine (◇) in serum are also shown. The control serum samples (5 μl) containing each ligand were diluted to 50 μl with a buffer solution (pH 7.0, 10 mM sodium cacodylate) containing PXT/TCA (5.0 μM), and then the fluorescence measurements were done. Excitation, 320 nm; detection, 367 nm. Temperature, 5°C. F and F_0 denote the fluorescence intensities in the presence and absence of target ligands, respectively. Errors are standard deviations obtained from three independent measurements at each concentration.

RNA aptamer has two internal loops that form the binding site and is able to discriminate caffeine on the basis of a 10^4-fold difference in the binding affinity [K_d (μM): theophylline, 0.32; caffeine, 3500; theobromine, >500]. The selective binding is explained by the formation of two hydrogen bonds between theophylline and cytosine, for which the N-7 hydrogen and C-6 keto oxygen of theophylline are critical. In the case of a 13-mer RNA aptamer with a relatively moderate binding selectivity [K_d (μM): theophylline, 13; caffeine, 590] (*35*), theophylline forms two hydrogen bonds with cytosine and uracil, where the N-7 hydrogen and N-9 nitrogen are involved in the binding.

In the present case, it is feasible that theophylline–cytosine binding is promoted by two hydrogen bonds involving the N-7 hydrogen and C-6 keto oxygen of theophylline (Figure 6(C)), similar to the binding in the 33-mer RNA aptamer (*33*, *34*). This explains the loss of binding affinity for caffeine and theobromine that have an additional methyl group at the N-7 position. Also, this binding mode would allow effective stacking with the adjacent 2-AP (Figure 6(C)), resulting in quenching upon theophylline binding.

The binding affinity of PXT/TCA is only moderate as compared to the 33-mer RNA aptamer (*33*, *34*), but it is strong enough for the detection of theophylline in serum samples. Here, a horse serum control sample containing theophylline (5 μl) was analysed after dilution with a buffer solution (45 μl, pH 7.0) that contained PXT/TCA. As shown in Figure 7, a linear response to theophylline is obtained in the concentration range from 5 to 20 μM, which corresponds to the concentration range from 50 to 200 μM in the original serum samples. PXT/TCA is thus applicable to the monitoring of serum theophylline concentration in the therapeutic range (60–100 μM) (*32*), and the analysis requires no further purification of serum samples such as deproteination.

Design of label-free signalling aptamers based on abasic site-binding fluorescent ligands

As described in the previous section, signalling aptamers possess considerable advantages in analytical assay for detecting molecules in solutions. An impressive number of designs for aptamer-based signalling systems have been so far proposed based on fluorescence, colorimetry and electrochemistry (*4*–*7*). While most approaches to this end have employed the covalent attachment of transducing elements to generate detectable signals from the binding events, we here describe a design strategy for label-free aptamer-based fluorescence-signalling systems (*19*, *20*).

The strategy utilised here is a kind of replacement assay with an abasic site-specific fluorescent ligand for which the abasic site is designed to be situated within the aptamer system, using another single-stranded DNA (*19*). An adenosine-binding DNA aptamer (*36*) was examined as a model system. As schematically illustrated in Figure 8, we prepared two kinds of DNA, a 32-mer aptamer (**AA1**: 5′-*AGAGA ACCTG GG*GGA GTATT GCGGA GGAAG GT-3′) and a 12-mer abasic site-containing DNA (**AC2**: 5′-CCCAG **X**TTCT CT-3′, **X** = abasic site). **AA1** is composed of a sequence of the reported 27-mer adenosine aptamer (*36*) (underlined bases of the **AA1** sequence) and an additional AGAGA sequence at the 5′-end. **AC2** has a sequence complementary to a part of the **AA1** sequence (bases written in italic), and it can form a duplex with **AA1** in the absence of target adenosine. The resulting **AA1/AC2** duplex has the abasic site in the double-stranded region, and therefore, the abasic site-specific ligand can bind to the duplex with fluorescence quenching. When the adenosine binding takes place, **AC2** is forced to dissociate from the **AA1/AC2** duplex, and aptamer **AA1** undergoes a conformational transition from an unfolded to a folded structure in which two adenosine molecules are trapped in the binding cavity. This adenosine binding also causes a release of abasic site-specific ligand from the **AA1/AC2** duplex, and its fluorescence is turned on.

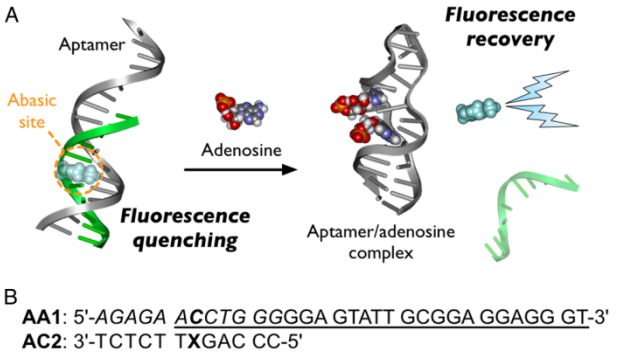

Figure 8. (A) Illustration of the label-free fluorescence-signalling system based on a combination of an adenosine-binding DNA aptamer, an abasic site-containing DNA and an abasic site-binding fluorescent ligand. (B) Names and sequences of DNAs examined in this study: X = abasic site (Spacer-C3, a propyl linker).

The key for the design of the proposed system is to use the abasic site-specific fluorescent ligands that have been found by us in order to develop fluorescence assay for SNP typing (*27*, *28*, *37*–*49*). These ligands are flat aromatic molecules having hydrogen bond-forming sites, including 2-amino-1,8-naphthyridines (*37*–*41*), pteridines (*42*–*45*), 3,5-diaminopyrazines (*46*, *47*), flavins (*27*, *28*, *48*) and 7-nitrobenzo-2-oxa-1,3-diazole derivatives (*49*). In contrast to typical DNA-binding ligands based on intercalation or groove binding, these ligands can bind selectively to the abasic site in DNA duplexes, where the binding is promoted by a pseudo-base pairing with intrahelical nucleobases opposite the abasic site and by stacking with nucleobases flanking the abasic site (Figure 9). Upon binding to the abasic site, the fluorescence of these ligands is usually quenched due to stacking with nucleobases flanking the abasic site as has been observed for fluorescent 2-AP. In this study, we utilised a 1,8-naphthyridine derivative, 2-amino-5,6,7-trimethyl-1,8-naphthyridine (ATMND, Figure 9) (*40*), due to its strong affinity for the abasic site (K_d = 53 nM at 20°C, pH 7.0, I = 0.11 M) and its high fluorescent quantum yield (0.54).

An examination of the sensing properties reveals a promising feature of the present system for adenosine

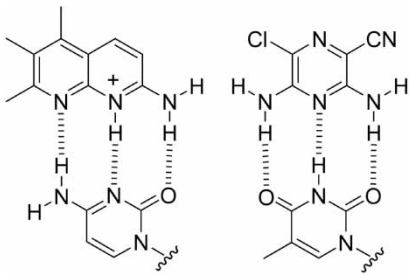

Figure 9. Chemical structures of abasic site-binding fluorescent ligands, ATMND and DCPC, utilised in this study, and their possible binding modes with nucleobases at the abasic site.

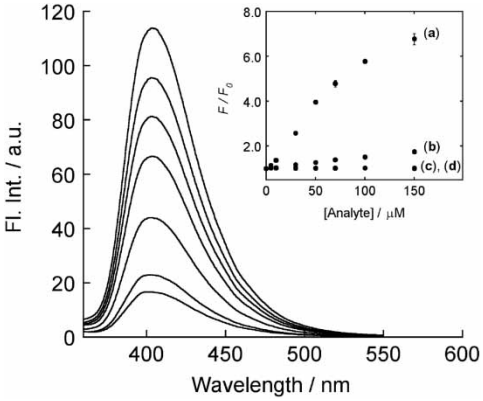

Figure 10. Fluorescence response of AA1/AC2/ATMND system to adenosine (0–150 μM) in solutions buffered to pH 7.0 (10 mM sodium cacodylate) containing 300 mM NaCl and 1.0 mM EDTA (*19*). [AA1/AC2 duplex] = 4.0 μM, [ATMND] = 2.0 μM. Excitation was at 350 nm and $T = 5$°C. Inset: responses of AA1/AC2/ATMND to (a) adenosine, (b) guanosine, (c) cytidine and (d) thymidine. F and F_0 denote the fluorescence intensities (403 nm) in the presence and absence of ligands, respectively.

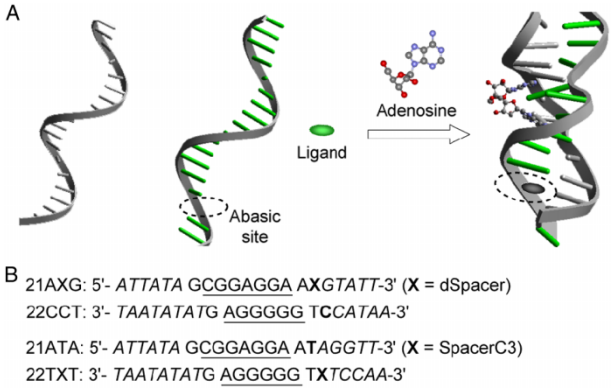

Figure 11. (A) Illustration of the label-free fluorescence-signalling system for adenosine based on a combination of a target binding-induced self-assembling DNA aptamer and an abasic site-binding fluorescent ligand. (B) Names and sequences of DNAs examined in this study: underlined sequences form a duplex having two bulge sites for the incorporation of adenosine; italic bases are complementary to each other.

detection. As shown in Figure 10, the fluorescence due to ATMND is clearly enhanced in the presence of adenosine, and the emission intensity at 403 nm recovers greatly to 6.8-fold after adding 150 μM adenosine. The response is concentration dependent in which the linear response is obtained in the concentration range from 5 to 100 μM (inset of Figure 10). By contrast, the responses to other nucleosides such as guanosine, cytidine and thymidine are only moderate or negligible (inset of Figure 10). Apparently, aptamer **AA1** does bind to adenosine without a loss of its inherent binding selectivity, and the proposed operating principle is effective to obtain a clear fluorescence signal.

A significant advantage of the present system can be seen from the comparison with aptamer-based adenosine sensors reported in some literatures. While the use of abasic site-containing **AC2** seems somewhat lower than the original binding affinity of adenosine-binding aptamer ($K_d = 6 \pm 3$ μM) (*36*), the detection limit of the present system for adenosine is estimated as 2 μM and it is superior to the reported optical detection systems, such as crosslinked (300 μM) (*50*) or non-crosslinked (10 μM) (*51*) gold nanoparticles, quantum dots (50 μM) (*52*) and DNAzyme-based colorimetric assay (6 μM) (*53*).

Another advantage of the present system is the response time to detect adenosine in solutions. While electrochemical sensors for adenosine with high sensitivity have been reported based on a ferrocene-labelled aptamer probe (detection limit: 20 nM) (*54*) or non-labelled aptamer probe (detection limit: ~100 nM) (*55*), it was reported that 90 min or 3 h was needed to obtain a stable response for the detection of adenosine (*54*, *55*). In our system, the response was very fast and reached a constant value within several minutes, and the fluorescence intensity of ATMND was very stable for more than 1 h.

Potential of the abasic site-specific fluorescent ligands for the design of label-free signalling aptamers was also demonstrated for another adenosine sensor (*20*). In this case, the reported sequence of adenosine aptamer (*36*) was divided into two fragments (DNA single strands). As schematically illustrated in Figure 11, an abasic site was inserted into one of the DNA strands near the adenosine-binding site and the other was a usual DNA sequence. Two DNA strands can exist as a single-stranded state, and in the presence of adenosine, two subunits are forced to form a compact aptamer–adenosine complex with an abasic site in the stem unit. This binding event can be therefore read out by the binding of abasic site-specific fluorescent ligands to the aptamer–adenosine complex for which signal-off and signal-on design is possible by the choice of suitable fluorescent ligands.

As shown in Figure 12(A), using ATMND, the system shows a quenching response to adenosine in the concentration range from 1 to 40 μM with a detection limit of 1 μM. The system can be easily switched from a signal-off response to a signal-on response using 3,5-diamino-6-chloro-2-pyrazine carbonitrile (DCPC, Figure 9) as a light-up fluorescent ligand (*47*), in which the system responses to adenosine with a detection limit of 2 μM (Figure 12(B)). For both systems, the observed signals are very clear and highly selective to adenosine, and the detection limits are superior to those of aptamer-based adenosine sensors based on optical detection systems (*50*–*53*).

Summary

In summary, we have demonstrated a new class of DNA aptamers in which abasic sites in the duplex were utilised

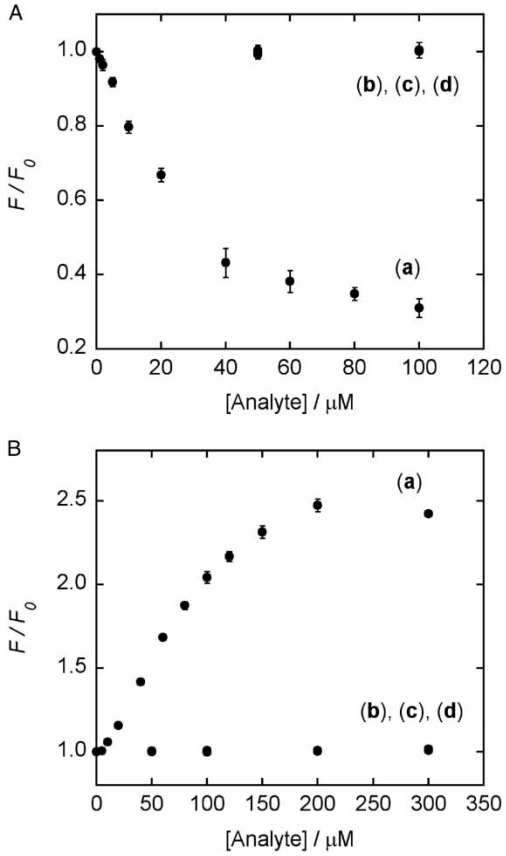

Figure 12. (A) Fluorescence responses to nucleosides in solutions buffered to pH 7.0 (10 mM sodium cacodylate) containing 300 mM NaCl and 1.0 mM EDTA: (a) adenosine, (b) guanosine, (c) cytidine and (d) thymidine (*20*). F and F_0 denote the fluorescence intensities in the presence and absence of ligands, respectively. $T = 5$°C. (A) 21AXG/22CCT/ATMND system: [DNA] = 1.0 μM, [ATMND] = 0.10 μM. Excitation, 350 nm; detection, 403 nm. (B) 21ATA/22TXT/DCPC system: [DNA] = 10 μM, [DCPC] = 5.0 μM. Excitation, 353 nm; detection, 412 nm.

as the active cavity for binding events. The abasic site-based flavin-binding aptamer showed a clear binding selectivity for riboflavin over FMN and FAD, and the binding affinity for riboflavin was comparable with binding affinities of RNA aptamers developed earlier for flavin binding. We have also developed a fluorescent signalling aptamer based on abasic site-containing duplex DNA that has a useful selectivity and sensitivity for the bronchodilator theophylline. The approach described here is straightforward, and further modification of the binding cavity by synthetic receptor and/or fluorescent nucleobases would be promising for the design of this class of DNA aptamers for a variety of small ligands.

In addition, we have demonstrated a design strategy for label-free aptamer-based fluorescence-signalling systems. We utilised an abasic site-specific fluorescent ligand and designed the abasic site to be situated within the aptamer system. The adenosine-binding aptamer was examined as a model system, and the resulting system was highly selective and sensitive with a considerable detection limit for adenosine. It is strongly expected that the design strategy proposed here has a wide application, and the use of abasic site-specific fluorescent ligands would offer a feasible approach to generate a signalling ability of a large variety of DNA- and RNA-based aptamers.

Acknowledgements

This work was partially supported by Grants-in-Aid for Scientific Research (A) (No. 17205009), Scientific Research (B) (Nos 18350039 and 20350032), Exploratory Research (No. 21655023) and the G-COE Project from MEXT, Japan. Partial support from CREST, Japan Science and Technology Agency (JST) is also acknowledged.

References

(1) Tuerk, C.; Gold, L. *Science* **1990**, *249*, 505–510.
(2) Ellington, A.D.; Szostak, J.W. *Nature* **1990**, *346*, 818–822.
(3) Hermann, T.; Patel, D.J. *Science* **2000**, *287*, 820–825.
(4) Willner, I.; Zayats, M. *Angew. Chem. Int. Ed.* **2007**, *46*, 6408–6418.
(5) Fischer, N.O.; Tarasow, T.M.; Tok, J.B.-H. *Curr. Opin. Chem. Biol.* **2007**, *11*, 316–328.
(6) Mairal, T.; Özalp, V.C.; Sánchez, P.L.; Mir, M.; Katalkis, I.; O'Sullivan, C.K. *Anal. Bioanal. Chem.* **2008**, *390*, 989–1007.
(7) de-los-Santos-Alvarez, N.; Lobo-Castanon, M.J.; Miranda-Ordieres, A.J.; Tunon-Blanco, P. *Trac – Trends Anal. Chem.* **2008**, *27*, 437–446.
(8) Sankaran, N.B.; Nishizawa, S.; Seino, T.; Yoshimoto, K.; Teramae, N. *Angew. Chem. Int. Ed.* **2006**, *45*, 1563–1568.
(9) Li, M.; Sato, Y.; Nishizawa, S.; Seino, T.; Nakamura, K.; Teramae, N. *J. Am. Chem. Soc.* **2009**, *131*, 2448–2449.
(10) Lindahl, T.; Nyberg, B. *Biochemistry* **1972**, *11*, 3610–3618.
(11) Krokan, H.E.; Standal, R.; Slupphaug, G. *Biochem. J.* **1997**, *325*, 1–16.
(12) Lindahl, T. *Nature* **1993**, *362*, 709–715.
(13) Hoeijmakers, J.H.J. *Nature* **2001**, *411*, 366–374.
(14) Friedberg, E.C. *Nature* **2003**, *421*, 436–440.
(15) Burgstaller, P.; Famulok, M. *Angew. Chem. Int. Ed.* **1994**, *33*, 1084–1087.
(16) Fan, P.; Suri, A.K.; Fiala, R.; Live, D.; Patel, D.J. *J. Mol. Biol.* **1996**, *258*, 480–500.
(17) Lauhon, C.T.; Szostak, J.W. *J. Am. Chem. Soc.* **1995**, *117*, 1246–1257.
(18) Roychowdhury-Saha, M.; Lato, S.M.; Shank, E.D.; Burke, D.H. *Biochemistry* **2002**, *41*, 2492–2499.
(19) Xu, Z.; Morita, K.; Sato, Y.; Dai, Q.; Nishizawa, S.; Teramae, N. *Chem. Commun.* **2009**, 6445–6447.
(20) Xu, Z.; Sato, Y.; Nishizawa, S.; Teramae, N. *Chem. Eur. J.* **2009**, *15*, 10375–10378.
(21) Chapman, S.K., Perham, R.N., Scrutton, N.S., Eds.; *Flavins and Flavoproteins*; Rudolf Weber Agency for Scientific Publications: Berlin, Germany, 2002.
(22) Müller, F., Ed.; *Chemistry and Biochemistry of Flavoenzymes*; CRC Press: Boca Raton, FL, 1991; Vol. 1.
(23) König, B.; Gallmeier, H.-T.; Reichenbach-Klinke, R. *Chem. Commun.* **2001**, 2390–2391.
(24) Tillotson, J.A.; Bashor, M.M. *Anal. Biochem.* **1980**, *107*, 214–219.

(25) Becvar, J.; Palmer, G. *J. Biol. Chem.* **1982**, *257*, 5607–5617.
(26) Caelen, I.; Kalman, A.; Wahlström, L. *Anal. Chem.* **2004**, *76*, 137–143.
(27) Nishizawa, S.; Sankaran, N.B.; Seino, T.; Cui, Y.-Y.; Dai, Q.; Xu, C.-Y.; Yoshimoto, K.; Teramae, N. *Anal. Chim. Acta* **2006**, *556*, 133–139.
(28) Sankaran, N.B.; Sato, Y.; Sato, F.; Rajendar, B.; Morita, K.; Seino, T.; Nishizawa, S.; Teramae, N. *J. Phys. Chem. B* **2009**, *113*, 1522–1529.
(29) Law, S.M.; Eritja, R.; Goodman, M.F.; Brealauer, K.J. *Biochemistry* **1996**, *35*, 12329–12337.
(30) Somsen, O.J.G.; van Hoek, A.; van Amerongen, H. *Chem. Phys. Lett.* **2005**, *402*, 61–65.
(31) Stivers, J.T. *Nucleic Acid. Res.* **1998**, *26*, 3837–3844.
(32) Hendeles, L.; Weinberger, M. *Pharmacotherapy* **1983**, *3*, 2–44.
(33) Jenison, R.D.; Gill, S.C.; Pardi, A.; Polisky, B. *Science* **1994**, *263*, 1425–1429.
(34) Zimmermann, G.R.; Jenison, R.D.; Wick, C.L.; Simorre, J.P.; Pardi, A. *Nat. Struct. Biol.* **1997**, *4*, 644–649.
(35) Anderson, P.C.; Mecozzi, S. *J. Am. Chem. Soc.* **2005**, *127*, 5290–5291.
(36) Huizenga, D.E.; Szostak, J.W. *Biochemistry* **1995**, *34*, 656–665.
(37) Yoshimoto, K.; Nishizawa, S.; Minagawa, M.; Teramae, N. *J. Am. Chem. Soc.* **2003**, *125*, 8982–8983.
(38) Satake, H.; Nishizawa, S.; Teramae, N. *Anal. Sci.* **2006**, *22*, 195–197.
(39) Morita, K.; Sato, Y.; Seino, T.; Nishizawa, S.; Teramae, N. *Org. Biomol. Chem.* **2008**, *6*, 266–268.
(40) Sato, Y.; Nishizawa, S.; Yoshimoto, K.; Seino, T.; Ichihashi, T.; Morita, K.; Teramae, N. *Nucleic Acids Res.* **2009**, *37*, 1411–1422.
(41) Ihara, T.; Uemura, A.; Futamura, A.; Shimizu, M.; Baba, N.; Nishizawa, S.; Teramae, N.; Jyo, A. *J. Am. Chem. Soc.* **2009**, *131*, 1386–1387.
(42) Yoshimoto, K.; Xu, C.-Y.; Nishizawa, S.; Haga, T.; Satake, H.; Teramae, N. *Chem. Commun.* **2003**, 2960–2961.
(43) Dai, D.; Xu, C.-Y.; Sato, Y.; Yoshimoto, K.; Nishizawa, S.; Teramae, N. *Anal. Sci.* **2006**, *22*, 201–203.
(44) Ye, Z.; Rajendar, B.; Dai, Q.; Nishizawa, S.; Teramae, N. *Chem. Commun.* **2008**, 6588–6590.
(45) Rajendar, B.; Rajendran, A.; Sato, Y.; Nishizawa, S.; Teramae, N. *Bioorg. Med. Chem.* **2009**, *17*, 351–359.
(46) Zhao, C.; Dai, Q.; Seino, T.; Cui, Y.-Y.; Nishizawa, S.; Teramae, N. *Chem. Commun.* **2006**, 1185–1187.
(47) Zhao, C.; Rajendran, A.; Dai, Q.; Nishizawa, S.; Teramae, N. *Anal. Sci.* **2008**, *24*, 693–695.
(48) Rajendar, B.; Nishizawa, S.; Teramae, N. *Org. Biomol. Chem.* **2008**, *6*, 670–673.
(49) Thiagarajan, V.; Rajendran, A.; Satake, H.; Nishizawa, S.; Teramae, N. *Chem. Bio. Chem.* **2010**, *11*, 94–100.
(50) Liu, J.; Lu, Y. *Angew. Chem. Int. Ed.* **2006**, *45*, 90–94.
(51) Zhao, W.; Chiuman, W.; Brook, M.A.; Li, Y. *Chem. Bio. Chem.* **2007**, *8*, 727–731.
(52) Liu, J.; Lee, J.H.; Lu, Y. *Anal. Chem.* **2007**, *79*, 4120–4125.
(53) Lu, N.; Shao, C.; Deng, Z. *Chem. Commun.* **2008**, 6161–6163.
(54) Wu, Z.-S.; Guo, M.-M.; Zhang, S.-B.; Chen, C.-R.; Jiang, J.-H.; Shen, G.-L.; Yu, R.-Q. *Anal. Chem.* **2007**, *79*, 2933–2939.
(55) Li, B.; Du, Y.; Wei, H.; Dong, S. *Chem. Commun.* **2007**, 3780–3782.